# An ancestral western diet causes transgenerational changes in offspring feeding behavior linked to alterations in brain mitochondrial proteome and microRNAs.

**Alexander Murashov** ( murashoval@ecu.edu )
East Carolina University
**Elena Pak**
East Carolina University
**Jordan Mar**
University of South Florida https://orcid.org/0000-0003-4597-2404
**Kelsey Fisher-Wellman**
East Carolina University https://orcid.org/0000-0002-0300-829X
**Krishna Bhat**
University of South Florida School of Medicine

**Article**

**Keywords:** western diet, exercise, obesity, mitochondrial proteome, food preference, miRNA, Drosophila

**Posted Date:** June 15th, 2022

**DOI:** https://doi.org/10.21203/rs.3.rs-1669761/v1

# Abstract

Parental lifestyle and eating habits are largely responsible for childhood obesity epidemic. Clustering of obesity in families suggests that cultural inheritance, genetics, and epigenetics work together to affect children's eating habits. In the current study, we explored whether epigenetic factors, such as ancestral diet, can influence offspring feeding behavior by using a fruit fly model. Here, we demonstrate that ancestral caloric overload alters offspring feeding behavior via transgenerational inheritance, along with changes in activity, triglyceride levels, and mitochondrial density in the brain. Mechanistically, we found that the generational differences are associated with changes in brain proteome and miRNA. The findings identify ancestral nutrition as a critical factor in the generational programming of feeding behavior.


# Introduction

Childhood obesity is a global public health problem associated with mounting health risks and increasing health care costs [1]. Studies have linked obesity to higher mortality rates, diabetes, hypertension, and metabolic syndrome, as well as depression, anxiety, and neurological disorders, including Alzheimer's disease, reviewed [2]. Obesity has been also associated with deficit in executive functions, suggesting dysfunction in the brain regions related to decision making, behavioral self-regulation, and reward-processing [3]. Consequently, food preferences and eating habits could become epigenetically hard-wired into the brain, intensifying overweight and obesity, and creating the perfect vicious cycle.

Ecological studies indicate that obesity clusters among individuals living in the same environment, with a tendency for the disease to run in families [4, 5]. Twin adoption studies and family aggregation studies suggest that body mass index (BMI) is highly inherited [6, 7]. However, single nucleotide polymorphisms (SNPs) could only explain less than 2% of the increased BMI in genome-wide association studies (GWAS) [7, 8]. A paradox therefore arises; how can the high heritability of obesity be explained if it does not correlate with a change in the DNA sequence?

A possible explanation comes from ecological studies in humans, such as the Dutch famine of WWII and the Overkalix studies, which indicate that poor ancestral diet can lead to metabolic risks through transgenerational epigenetic inheritance. [9, 10, 11, 12]. From Drosophila to rodents, researchers found that ancestral nutrition affected the offspring's metabolic and behavioral traits up to a fourth generation (reviewed [13, 14]). A particular focus has been on paternal effects, seeking to narrow down the possible transmission mechanisms to those mediated by germ cells (reviewed [13, 15, 16, 17]).

Paternal inter- and transgenerational effects have been documented in laboratory rodents after paternal fasting [18], exercise [19, 20], a low-protein diet [21], a high-fat diet [22, 23], and in human populations due to paternal diabetes [24, 25]. In *Drosophila*, inter- and transgenerational inheritance of metabolic traits has been documented in response to specific dietary ingredients such as sugar [26 27, 28], yeast protein [29], fat [30, 31, 32], a dilution of the standard diet [31], ethanol exposure [33], behavioral stress [34, 35], and genetic

manipulation of parental metabolism [36]. However, despite all the information accumulated over the last decade about metabolic risks inherited from generations to generations, we are still uncertain about how ancestral diet influences feeding behavior.

In this manuscript, we focused on paternal effects in order to narrow the range of potential mechanisms to those transmitted through sperm. Here we show that ancestral Western diet (WD) produces an increase in the offspring's feeding behavior, with concomitant decrease in locomotor activity, alterations in triglycerides, and mitochondrial density. Mechanistically, we find these changes to be associated with proteome remodeling, and alterations in miRNAs. The findings identify ancestral nutrition as a contributory factor in programming obesity-risk behaviors and could provide better insight into mechanisms of the familial susceptibility to obesity and the obesity pandemic in general.

# Methods

## 2.1 Drosophila culture

Flies used in all experiments were derived from a colony established from Drosophila simulans isofemale lines and maintained as an outbred population [37]. For transgenic experiments the following lines were acquired from Bloomington Drosophila Stock Center: 7009, 35014, 61377 and Canton-S. The fly stocks were maintained on the standard Bloomington Formulation diet (Nutri-Fly® BF, Cat #: 66–112, Genesee Scientific Inc., San Diego, CA) in a climate-controlled environment at 24°C under a 12h light-dark cycle and 65–70% humidity. All experiments were performed on age-matched 3-4-day old flies. All flies, from the embryo stage, were raised on the standard Nutri-Fly Bloomington diet (CD). The WD was based on the standard Nutri-Fly Bloomington diet with the addition of Nutiva USDA Certified Organic, non-GMO, Red Palm Oil (15% by weight), 15% Sucrose, and 0.1M NaCl as described previously [37].

The F1 offspring were generated by crossing exercise and diet-exposed males to control virgin females. The density was controlled by keeping breeding conditions constant for all groups and generations: 5 males and 5 virgins were bred. Briefly, to ensure a common parental larva density and epigenetic background, 0–4 days old flies were manually sorted to 5 males and 5 virgin females per vial and allowed to lay eggs for 48 hours in a wide vial at 24˚C, 70% humidity, and a 12-hour light cycle 3 days. F2-F4 offspring were generated in the same manner by breeding 5 males and 5 female siblings. Once vial begin to produce flies, the flies were collected within the four-day window. Flies, from the embryo stage, were raised on the standard Nutri-Fly BF diet. Each breeding group consisted of 10–20 breeding vials and N number for offspring statistics were based on a number of the breeding vials. The offspring were tracked with respect to the specific parental flies to prevent any given parent from dominating the pool. Each group of parental flies was represented by an equal number of offspring in each experiment.

## 2.2 Behavioral experiments

Locomotor activity was studied using LAM25H locomotor activity monitors (TriKinetics Inc, Waltham, MA) as described previously[37]. Briefly, the activity was measured in groups of five flies housed in narrow

vials with food with 3–4 replicates per diet. For flight exercise groups of sixty 3–4 old days, male flies were housed in 1-gallon clear plastic fish bowls (Petco, San Diego, CA) attached to a motorized platform. The bowls were shaken every 5 min daily for 7 h for 5 days as described previously[37].

## 2.3 Assays for triglycerides.

For dry weights, flies were killed in liquid nitrogen and then dried at 52ºC for 72 hours. Flies were individually weighed using Cahn C-35 Ultra-Microbalance (Thermo Fisher Scientific, Waltham, MA). The assays to measure triglycerides were carried out according to our published procedure [37]. Briefly, 5 flies were rapidly homogenized in 0.15 ml of PBST (PBS with 0.1% Tween 20) using Bullet Blender (Next Advance, Inc., Troy, NY). The samples were centrifuged for 3 min at a maximum speed at 4°C. Total proteins were measured using the Pierce Rapid Gold BCA Protein Assay Kit (A53225, Thermo Fisher Scientific). The assays for triglycerides were performed using incubations with Pointe Scientific Triglycerides Reagent (T7532120, Thermo Fisher Scientific). Triglyceride contents were normalized to mean fly weight and to total protein levels per mean fly weight.

## 2.4 Western blot analysis

The procedures followed those described previously [37]. Tissues (dissected flight muscle or head) were extracted and homogenized in Extraction Buffer (20 mM Tris-HCl pH 7.5, 5 mM Magnesium Acetate, 1 mM EDTA pH 8.0, 1 mM DTT, 1 mM PMSF in isopropanol, 1x PIC (Sigma Aldrich P2714), 0.5% Nonidet 40) for one minute on ice using a hand-held homogenizer (Bel-Art). The homogenate was then centrifuged at 13,000 rpm 5 minutes 4°C (Beckman). Volumes equivalent to one head/flight muscle were run through a 4–12% Bis-Tris precast gel (Invitrogen) and proteins were transferred to a 0.2µM nitrocellulose membrane (Bio-Rad). Membranes were then blocked in 25 mL 1x TBST (Tris Buffered Saline 0.1% Tween-20) + 5% powdered milk and incubated in 5 mL of primary antibody solution. All secondary antibodies were diluted 1x TBST + 1% powdered milk. Membranes were then incubated in Immobilon™ Western Chemiluminescent HRP Substrate (MilliporeSigma) according to manufacturer's directions and imaged using an Amersham Imager 600 (GE Healthcare Life Sciences). Primary antibodies used include CoxIV (mouse, 1:2000 or 1:5000, Abcam), ATP5a (mouse, 1:20,000, Abcam), Actin (mouse, 1:2500, Abcam), Actin (rabbit, 1:2500, Abcam), Tubulin (rabbit, 1:5000, Abcam), Ref2p (rabbit, 1:800, Abcam), ChAT4B1 (mouse, 1:500, DSHB). Secondary antibodies used include horseradish peroxidase-conjugated Donkey anti-Mouse (1:10,000, Jackson Laboratories) or Goat anti-Mouse (1:20,000, Jackson Laboratories) secondary antibodies.

## 2.5. FLIC

Fly Liquid-Food Interaction Counter (FLIC) system was utilized to monitor consumption of 10% sucrose solution according to the protocol described elsewhere[38, 39]. Flies were removed from their food environment and loaded onto Drosophila Feeding Monitor (DFM), using a flight aspirator. Fly feeding behavior was monitored continuously for 24 h starting at 12 pm. FLIC data were analyzed using R studio (https://www.rstudio.com/) and custom R code, which is available at

https://github.com/PletcherLab/FLIC_R_Code. Default settings were used for analysis. Wells that had zero feeding events over the testing interval were removed from the analysis.

# 2.6 Proteomics

*Sample prep for label-free proteomics*

Fly brains were quickly dissected on ice cold block and frozen on dry ice. Isolated fly brains were lysed in urea lysis buffer (8M urea in 40mM Tris, 30mM NaCl, 1mM $CaCl_2$, 1 x cOmplete ULTRA mini EDTA-free protease inhibitor tablet; pH = 8.0), as described previously[40, 41]. The samples were subjected to three freeze-thaw cycles, and sonication. Samples were centrifuged at 10,000 x g for 10min at 4°C. Protein concentration was determined by BCA. Equal amounts of protein were reduced with 5mM DTT at 37°C for 30min, and then alkylated with 15mM iodoacetamide for 30min in the dark at room temperature. Unreacted iodoacetamide was quenched with DTT (15mm). Initial digestion was performed with Lys C (ThermoFisher Cat# 90307; 1:100 w:w) for 4hr at 32°C. Following dilution to 1.5M urea with 40mM Tris (pH = 8.0), 30mM NaCl, 1mM $CaCl_2$, samples were digested overnight with trypsin (Promega; Cat# V5113; 50:1 w/w) at 32°C. Samples were acidified to 0.5% TFA and then centrifuged at 4,000 x g for 10min at 4°C. As described previously[40], supernatant containing soluble peptides was desalted, and then eluate was frozen and subjected to speedvac vacuum concentration.

*nLC-MS/MS for label-free proteomics*

Final peptides were resuspended in 0.1% formic acid, quantified (ThermoFisher Cat# 23275), and then diluted to a final concentration of 0.25µg/µL. Samples were subjected to nanoLC-MS/MS analysis using an UltiMate 3000 RSLCnano system (ThermoFisher) coupled to a Q Exactive Plus Hybrid Quadrupole-Orbitrap mass spectrometer (ThermoFisher) via a nanoelectrospray ionization source. For each injection, 4µL (1µg) of sample was first trapped on an Acclaim PepMap 100 20mm × 0.075mm trapping column (ThermoFisher Cat# 164535; 5µL/min at 98/2 v/v water/acetonitrile with 0.1% formic acid). Analytical separation was performed over a 120min gradient (flow rate of 250nL/min) of 4–45% acetonitrile using a 2µm EASY-Spray PepMap RSLC C18 75µm × 250mm column (ThermoFisher Cat# ES802A) with a column temperature of 45ºC. MS1 was performed at 70,000 resolution, with an AGC target of $3x10^6$ ions and a maximum injection time (IT) of 100ms. MS2 spectra were collected by data-dependent acquisition (DDA) of the top 15 most abundant precursor ions with a charge greater than 1 per MS1 scan, with dynamic exclusion enabled for 20s. Precursor ions isolation window was 1.5m/z and normalized collision energy was 27. MS2 scans were performed at 17,500 resolution, maximum IT of 50ms, and AGC target of $1x10^5$ ions.

*Data analysis for label-free proteomics*

As described previously [40], with some modification, Proteome Discoverer 2.2 (PDv2.2) was used for raw data analysis, with default search parameters including oxidation (15.995 Da on M) as a variable modification and carbamidomethyl (57.021 Da on C) as a fixed modification. Data were searched against

the Uniprot Drosophila melanogaster reference proteome (Proteome ID: UP000000803). Both reviewed (Swiss-Prot) and unreviewed (TrEMBL) were included. PSMs were filtered to a 1% FDR and grouped to unique peptides while maintaining a 1% FDR at the peptide level. Peptides were grouped to proteins using the rules of strict parsimony and proteins were filtered to 1% FDR. Peptide quantification was done using the MS1 precursor intensity. Imputation was performed via low abundance resampling.

*Statistical evaluation*

All proteomics samples were normalized to total protein abundance, and the protein tab in the PDv2.2 results was exported as a tab delimited .txt. file and analyzed. Protein abundance was converted to the $Log_2$ space. For pairwise comparisons, tissue mean, standard deviation, p-value (p; two-tailed Student's t-test, assuming equal variance), and adjusted p-value (Benjamini Hochberg FDR correction) were calculated [42, 43]. All raw data are available online using accession number "xxx" for jPOST Repository [44, 45].

# 2.7 miRNA PCR

Total RNA was isolated from frozen tissues by standard methods [46] and then was used for cDNA synthesis and subsequent qRT-PCR. Flight muscles, brains and sperm were quickly isolated on wet-ice metal blocks from cold-anesthetized flies. Sperm isolation followed previously described protocol[26]. Total RNA from tissue samples was extracted with an RNAqueous MicroScale RNA Isolation Kit according to the manufacturer's instructions (Thermo Fisher–Life Technologies, Grand Island, NY, USA). Polyadenylation and reverse transcription were performed using Takara microRNA first-strand synthesis and miRNA quantification kit (#638313). Equal concentrations of total RNA from 5 muscles, 10 brains or 20 individual sperm samples were used to produce 3 RNA pools per group. Real-time PCR reactions on micro-RNA (miR) were carried out using TB Green Advantage qPCR Premix kit (#639676, Takara) in triplicates for each cDNA sample on QuantStudio 6 Flex PCR System (Thermo Fisher). Primers specific for each miRNA and mRNA were obtained from Invitrogen. As internal controls, primers for U6 (the noncoding small nuclear RNA), and miR-191 were added for RNA template normalization, and the relative quantifications of miRNA expression were calculated against miR-191 by the $\Delta\Delta C_t^2$ method. Constitutively expressed miR-191 was used as a normalization control for miRNA qPCRs. The experiments were performed 3 times independently.

# 2.8 Mitochondrial copy numbers

DNA from 5 flight muscles or 10 brains of adult flies were purified using Purigen Core Kit A (Qiagene) according to manufacturer's protocol. Briefly, tissue was sonicated in 80 µl of cell lysis buffer, incubated at 65°C for 15 min, quickly cooled down and 27ul of protein precipitation solution was added. Samples were incubated on ice and then centrifuged at 13,000–16,000g for 3 min. Supernatants were precipitated with isopropanol and centrifuged at 13,000–16,000g for 5 min, pellet was then carefully washed with 70% ethanol two times, air dried and resuspended in 12.5 ul of Hydration solution. DNA concentration was measured by nano-drop spectrophotometry and samples were diluted to 20 ng/ul.

Relative DNA levels of rpol2 (single-copy nDNA) and mt:lRNA (16S, mtDNA) were determined by qPCR using TB Green Advantage qPCR Premix (TaKaRa), using as template 1 ul of DNA in a 10ul reaction, together with gene-specific primer pairs each at 500 nM, as follows (all shown 5' to 3'): rpol2 AGGCGTTTGAGTGGTTGG and TGGAAGGTGTTCAGTGTCATC, mt_lRNA AGTCTAACCTGCCCACTGAA and CCAACCATTCATTCCAGCCT. mtDNA copy number was calculated from the cycle-time difference (ΔCT) of the two genes, using the formulas described previously [47]: ΔCT = (nucDNA CT – mtDNA CT); relative mitochondrial DNA content = 2 × 2ΔCT.

# 2.9 Statistics

Statistical analyses were done with student t-test, Mann–Whitney *U* test, a one-way and two-way ANOVA, depending on the particular data set using GraphPad Prism version 8.00 for Windows, (GraphPad Software, San Diego, CA). Post hoc analyses were conducted using Tukey's test.

## Results

The human WD consists of highly palatable, high-salt, high-fat, and high-sugar, energy-dense foods [48]. This diet imitated in rodent studies and often dubbed as a "cafeteria diet" results in rapid weight gain, glucose and insulin intolerance, with concomitant alterations in neuronal signaling involved in the control of feeding behavior [49, 50, 51, 52]. While several “cafeteria diets” have been developed for rodents [53], to the best of our knowledge, no such diet has been developed for *Drosophila*. As a first step toward filling this knowledge gap, we have recently created a diet with increased fat, sugar, and salt for *Drosophila* called the Western diet (WD) [54].

For this study we used *D. simulans*, which was successfully used to characterize effects of WD previously [37].

# 3.1 Ancestral WD causes increase in offspring feeding behavior up to the fourth generation.

To begin to explore whether ancestral diet may alter offspring feeding behavior, paternal male flies were subjected to the WD or the WD plus exercise. Two other groups included sedentary flies on the CD and the CD plus exercise. The effect of ancestral diet on male and female flies of F1-F4 generations was studied using Fly Liquid-Food Interaction Counter (FLIC), which allows high-throughput, continuous analysis of feeding behaviors [38]. Specifically, FLIC allows to measure feeding behaviors by detecting electronic signals, “licks,” when the fly proboscis touches the food. Flies were removed from their food environment and gently loaded onto Drosophila Feeding Monitor (DFM), using a flight aspirator. Feeding reservoirs were filled with 10% sucrose solution. Fly feeding behavior was monitored continuously for 24 h starting at 12 pm.

The offspring groups included control father offspring (CFO), exercised father offspring (EFO), WD father offspring (WFO), WD + exercise father offspring (WEFO). The assay showed that both male and female WFO offspring had significantly more licks than other groups. This increase was observed in F1-F4 male flies and F2-F4 female flies according to one-way ANOVA (Fig. 1. A, B). The significant increase in licks was observed in F2, F4 males and F3-4 females in comparison to CFO lineage. In F1, F3 males and F2 females the increase in feeding was significant in comparison to exercise lineages EFO and WEFO. In F4 females the increase in feeding was significant against WEFO. Paternal exercise led to decrease in feeding behavior in F3 males and F2 females, and to increase in F3, F4 females. Interestingly, combination of paternal WD and exercise in negated effect of WD in F1, F3, F4 males and F2, F4 females of WEFO lineage. The findings of this study suggest that ancestral WD causes transgenerational increase in offspring feeding behavior while ancestral exercise counterbalances this effect.

Increase in food consumption leads to obesity with concomitant increase in biochemical markers. In the following experiment we performed biochemical assays to assess if transgenerational increase in offspring feeding behavior altered level of triglycerides (Fig. 1C). The experiment revealed that level of triglycerides in whole body homogenate was the highest in WF flies and lowest in EF animals. Ancestral exercise significantly negated the impact of WD, reducing the triglycerides in WEF flies compared with control. Taken together, these data show that ancestral WD leads to obesity in offspring.

## 3.2 Ancestral WD negatively impacts locomotor activity and muscle and brain mitochondrial enzymes.

Generally, increased food consumption and triglycerides have a negative impact on physical activity, so next we asked if ancestral experiences affected the activity of offspring. The activity of male and female offspring was recorded over 5-day period using LAM25H locomotor activity monitors (TriKinetics). The experiments showed that in male WFO offspring the activity was significantly increased in the F1 but decreased in F2-F4 (Fig. 1D). In contrast, activity in EFO offspring was higher in F1-F3 and decreased in F4. The activity of WEFO offspring was significantly lower than WFO in F1-F3 but higher in F4.

In female offspring, the activity of WFO group was significantly decreased in F1-F4, while EFO activity was higher in F1 and lower in F3-F4 (Fig. 1E). WEFO activity was higher than WFO in F2-F4. Thus, according to these data, WD causes a transgenerational decline in locomotor activity in both sexes.

Locomotor activity relies on muscle bioenergetics including efficiency in oxidative phosphorylation (OXPHOS) efficiency, and activity of individual enzymes in the mitochondrial electron transport chain (ETC). To investigate whether offspring alterations in locomotor activity were due to deficiency in mitochondrial OXPHOS, we performed western blot analysis for Cox4 (cytochrome c oxidase or Complex IV) and ATP5A, a subunit of the catalytic portion of the ATPase, also known as Complex V. The experiments showed that both Cox4 and ATP5A were significantly downregulated in flight muscle of F1 WFO males, suggesting compromised mitochondrial function (Fig. 2A, B, SI Fig. 1). The brain western blots did not reveal any statistically significant differences (SI Fig. 1).

## 3.3 Decreased mitochondrial density in muscles and the brain due to ancestral WD

Ancestral diet could affect bioenergetic phenotype in several ways epigenetically, including reducing metabolic capacity through changes in mitochondrial density [55]. A decrease in mitochondrial density would lead to a reduction in ATP-producing sites, making cells less energy efficient and susceptible to metabolic disorders [56]. In the following experiment, we investigated whether ancestral WD affected mitochondrial copy number (MCN) using qPCR approach [57]. MCN was studied in brain and fly muscle of parental and offspring flies. The experiments showed that MCN levels were significantly lower in brains and muscles of WD-fed fathers (WF) (Fig. 2C). Interestingly, exercise mitigated the negative effect of WD in WEF group and increased the amount of MCN in muscles from exercised fathers (EF). In offspring groups, the ancestral WD decreased MCN in both brains and muscles of F1-F4 WFO males(Fig. 2D, E). The decrease of MCN was less pronounced in female offspring reaching statistical significance in F2 brains and F1, F3 muscles. This data show that ancestral WD and exercise have transgenerational programming effects on brain and muscle mitochondrial density and consequently these tissues bioenergetics.

## 3.4 Paternal WD causes deregulation of F1 brain proteome.

Several lines of evidence indicate that obesity induces changes in brain proteomics [58]. It is less well understood, however, how ancestors' diets might affect offspring's brain proteins. To begin to explore whether ancestral WD may impact offspring proteome, nLC-MS/MS was used to interrogate the proteome of F1 offspring brain. This approach yielded 2,802 proteins identified and quantified across all samples. Importantly, the top 10 most abundant proteins corresponded to known mitochondrial membrane and cytoskeletal proteins (ATP5a, betaTub56D, ATPsynβ, porin, alpha-Spec, Gs2, mAcon1, sesB, Adh, PyK). ATP5a synthase abundance was identical across offspring lineages, confirming equal total amounts of protein across samples (Fig. 3). Using a P value less than 0.01 cutoff we have identified 74 differentially expressed proteins comparing WFO to CFO in males, and 70 differentially expressed protein comparing WFO to CFO in females, 28 differentially expressed proteins comparing EFO to CFO in males, and 34 differentially expressed protein comparing EFO to CFO in females, and 125 differentially expressed proteins comparing WEFO to CFO in males, and 103 differentially expressed protein comparing WEFO to CFO in females (Fig. 4, SI Fig. 2 Heat map, SI Excel table1). Metascape Gene Analysis (https://metascape.org) showed a significant enrichment in terms related to translation and translation factors, small molecule metabolic process, purine metabolism, Rho GTPases, and carbohydrate metabolism (Fig. 4B, D, F, H, J, L). The TCA cycle and ETC were among downregulated pathways in both WFO and WEFO males (SI Fig. 2). In WFO females the downregulated proteins were associated with "small molecule metabolic process", "vesicle-mediated transport in synapse", and "cellular homeostasis". Upregulated proteins were related to "metabolism of RNA", "translation", and "heterochromatin organization"(SI Fig. 3).

Using a 2-fold cutoff, we discovered that Huntingtin (Htt) was downregulated in both WFO and WEFO female (see volcano plots Fig. 4C, K). Htt is the ortholog of human HTT. It encodes a scaffold protein involved in mitotic spindle orientation, chromatin regulation and axonal transport[59, 60]. Interestingly, dHYPK- an ortholog to human huntingtin interacting protein K was 3.6-fold down in WEFO males (volcano plot Fig. 4I). Among upregulated proteins, mei-P26 (meiotic P26) was elevated in both WFO and WEFO males and WEFO females (volcano plots, Fig. 4A, I, K). Recent observations indicate that mei-P26 regulates translational repression by inhibiting the microRNA pathway [61, 62].

## 3.5 The evolutionary conserved miRNA mir-10 is identified as a potential epigenetic regulator by miRNA target prediction

Growing evidence suggests that miRNAs play significant role in inheritance of transgenerational phenotype [63, 64]. To determine if miRNA might be involved in regulating proteomic changes in the brain, web tool MIENTURNET (MicroRNA ENrichment TURned NETwork)[65] was used for miRNA-target enrichment analysis. The tool uses TargetScanFly 7.2 to locate evolutionarily conserved microRNA binding sites. The analysis was performed on subset of proteins with significant enrichment for terms related to translation, small molecule metabolic processes, and carbohydrate metabolism. The results showed that mir- 277-3p, mir-10-3p and mir-927-5p had the highest number of predicted targets (Fig. 5A, B). In turn, mei-P26 contained the highest number of conserved sites for miRNAs including mir- 277-3p, mir-10-3p and mir-927-5p (Fig. 5C). To assess miRNA regulatory roles and identify controlled pathways, we used DIANA-tools mirPath v.3 (www.microrna.gr). Based on unbiased empirical distributions and meta-analysis statistics, this tool performs functional annotation of one or more miRNAs[66]. The MirPath analysis identified "Purine metabolism" as a pathway targeted by all three miRNAs: mir-277-3p, mir-10-3p, and mir-927-5p (Fig. 5D). We chose miR-10 for study because, among three, it is the only miRNA conserved in bilaterian animals, including humans [67]. miR-10 has been implicated in variety of epigenetic processes including cancer, regulation of Hox translation [68] and control of cell differentiation [69].

## 3.6 The expression of Mir-10 in brain and spermatozoa is controlled by paternal WD

In several studies, sperm miRNA has been identified as a carrier of epigenetic information. [63, 64, 70]. In order to investigate whether miR-10-3p could mediate transgenerational phenotype, we examined expression of mir-10 in brain and sperm by qRT-PCR.

As shown in Fig. 6A, several miRNAs including miR-10-3p were upregulated in brains of WF fathers and their offspring. Interestingly, miR-10-3p was increased in female offspring but not male offspring. qRT-PCR on purified spermatozoa revealed significant increase of several miRNAs including miR-10-3p in paternal and offspring spermatozoa (Fig. 6B). Several miRNAs including mir-277-3p were undetectable in

spermatozoa. This data suggests that miR-10-3p could potentially mediate transgenerational phenotype in a fruit fly model.

# 3.7 Knock-down of miR-10 increases feeding behavior.

To begin to elucidate if miR-10-3p could be responsible for transmission of transgenerational phenotype we used the UASxGAL4 strategy to induce UAS-miR10 lines with dopa decarboxylase (Ddc)-GAL4 driver. Ddc-Gal4 encodes the promoter region of the DDC gene, which is involved in the serotonin and dopamine synthesis, and its expression is associated with dopaminergic and serotonergic neurons, which are responsible for both aversive and appetitive behaviors[71]. We used two RNAi lines (35014 and 61377) targeting miR-10, thus avoiding potential off-target effects associated with a particular construct. 35014 expresses dsRNA for RNAi of mir-10 (FBgn0262424) under UAS control in the VALIUM20 vector. 61377 expresses an antisense 'sponge' RNA under UAS control for knocking down mir-10 expression. For control, we used the parent lines or F1 cross to Canton-S (CS). The analysis of the of F1 feeding behavior using FLIC showed that both male and female flies had significant increase in feeding behavior (Fig. 6C). The biochemical assay revealed an increase in total body triglycerides in males and a strong trend in female offspring (Fig. 6D). qRT-PCR in the brains demonstrated a reduction in miR-10-3p in 7009x35014 confirming successful knockdown (Fig. 6E).

In sum, these findings suggest that miR-10 might act as an epigenetic factor modulating feeding behavior.

# Discussion

Our recent observations documented that a combination of saturated fat, sugar, and salt in WD significantly shortens lifespan, decreases locomotor activity, impairs learning and memory and compromises reproductive function more so than any of the ingredients individually [37, 72]. Daily flight exercise negated effects of WD. Remarkably, the WD was preferred over control food despite its harmful outcomes, suggesting that these preferences could be hard-wired[37]. As feeding behavior is a key factor in obesity and metabolic disorders, our goal in the present study was to determine whether the WD can have intergenerational effects on feeding behavior of offspring.

### 4.1 Ancestral WD causes transgenerational increases in feeding behavior, triglyceride levels, with concomitant decrease in locomotor activity and mitochondrial function.

The transgenerational metabolic effects of caloric overload have been previously reported in Drosophila [26, 32], rodents [22, 23, 73] and humans [24, 25]. However, to the best of our knowledge this is the first report documenting transgenerational effect of ancestral diet and exercise on feeding behavior. Our experiments revealed that paternal WD increases feeding behavior up the 4th generation. Remarkably, ancestral WD also increased triglycerides and decreased locomotor activity in male and female offspring while ancestral exercise tended to mitigate these effects. The causes for transgenerational increase in triglycerides is not clear but could be due to combination of factors including overeating, being a "couch

potato" or changes in cellular metabolism. Interestingly, study of OXPHOS enzymes revealed a marked decrease in levels of Cox4 and ATP5 in male flight muscle suggesting epigenetic alterations to mitochondrial bioenergetics. In addition, WD was associated with significant reductions in mitochondrial copy numbers both in paternal, and offspring muscle and brain. This data are supported by previous observations on decrease in mitochondrial complexes [74], and mitochondrial copy number after caloric overload in flies [75] as well as inheritance of mitochondrial dysfunction over three generations in mice [73]. In the current study, the effect of ancestral WD was somewhat more pronounced in male offspring. While the reason for this is unclear it could be due to females having higher reproductive needs and correspondingly metabolic demands. Females have been proposed to have higher "metabolic flexibility", allowing them to switch more easily between glycolysis, beta-oxidation of fatty acids, and amino acid oxidation as sources of energy and substrates for mitochondrial respiration[76].

### 4.2 Ancestral experiences affect offspring brain proteome

Alterations in mitochondrial density and feeing behavior have been associated with significant proteomic changes in the brain. Both WD and exercise produced significant changes in protein levels with associated enrichment for GO terms and pathways related to translation and translation factors, small molecule metabolic process, purine metabolism, Rho GTPases, and carbohydrate metabolism in both males and female's offspring. Amid downregulated pathways in both WFO and WEFO males were bioenergetic processes such as TCA cycle and ETC. Among downregulated proteins in WFO and WEFO females was htt and dHYPK in WEFO males. Both proteins are fly orthologs of human proteins related to Huntington's' disease (HD). Although the exact function of htt protein is not well understood it plays an important role in embryonic development, nerve cells signaling and axonal transport[77]. HYPK- an interaction partner of HTT, is an intrinsically disordered protein involved in chaperone activity in protein folding, cell cycle arrest, anti-apoptosis and transcription regulation [78, 79]. Moreover, recent report showed that hypothalamic expression of mutant htt causes distinct metabolic changes in HD mice including weight gain and decrease in locomotor activity suggesting the role of HTT in metabolic control via hypothalamic neurocircuits.[80]. Amongst upregulated proteins, mei-P26 was elevated in both WFO and WEFO males and WEFO females. mei-P26 is involved in meiosis, germline differentiation and spermatogenesis[81, 82]. It is part of the RNA-induced silencing complex (RISC) and controls translational repression by inhibiting the microRNA pathway [61, 62].

miRNAs play significant role in regulation of protein expression, establishing epigenetic memory [83], and transgenerational phenotype [63, 64]. Using MIENTURNET [65] for miRNA-target enrichment analysis we identified mei-P26 as a top target with over 25 conserved sites for miRNAs. Next, mir-277-3p, mir-927-5p, and mir-10-3p were identified as miRNAs targeting the most proteins associated with GO terms for translation, small molecule metabolic process, and carbohydrate metabolism. Interestingly, DIANA-tools mirPath identified that all three miRNAs target purine metabolism a pathway critical for cell growth, division and energy production[84]. In addition, miR-277 affects branched-chain amino acid catabolism and lifespan in flies (Esslinger et al., 2013) while miR-927 controls fly developmental growth by targeting

Krüppel homolog1 (Kr-h1)(He et al., 2020). Amongst the three top miRNAs miR-10 is the most interesting as it is highly conserved in a diverse range of bilaterian animals including humans, resides in homeobox gene cluster(Tehler et al., 2011) and involved in several epigenetic processes including development and cell differentiation (Wang et al., 2021). Mir-10 was also identified as a spermatozoal miRNA involved in transgenerational phenotypic changes. Among small RNA species, miR-10 was one of the most upregulated by paternal obesity in the sperm of F1 male mice[85]. In our unpublished RNA-seq data miR-10 was also a top spermatozoal miRNA regulated by exercise in a mouse model of thrifty phenotype (Murashov, unpublished observation).

**4.3 miR-10 in modulating feeding behavior.**

To investigate whether miR-10-3p could mediate transgenerational phenotype, we examined expression of mir-10 in brain and sperm by qRT-PCR. miR-10-3p showed WD-regulated pattern of expression in brains of fathers and female offspring. miR-10-3p was also increased in fathers and male offspring spermatozoa suggesting that miR-10 could potentially mediate transgenerational phenotype. We used the UASxGAL4 strategy to induce UAS-miR10 lines with Ddc-GAL4 driver. Ddc-Gal4 encodes the promoter region of the DDC gene, which is expressed in dopaminergic and serotonergic neurons associated with both aversive and appetitive behaviors. The analysis of the of F1 feeding behavior using FLIC revealed that both male and female flies had significant increase in feeding behavior. The biochemical assay revealed an increase in total body triglycerides in F1 offspring. qRT-PCR on the brains also demonstrated a reduction in miR-10-3p, confirming successful knockdown. These findings indicate that miR-10 might play a mechanistic role in transmitting paternal lifetime experiences across generations.

The exact mechanism of transgenerational transmission remains to be determined, but it may be that ancestral caloric overload causes mitochondrial inefficiency followed by compensatory proteome remodeling followed by later decompensation with dysregulation of miRNAs. Consequently, miRNAs act as information carriers that transmit phenotypic traits from generation to generation. In the germline, miRNAs affect development, resulting in proteomic changes and mitochondrial dysfunction, which leads to behavioral compensations such as overeating and preference for energy-dense foods, creating a perfect vicious cycle. (Fig. 7).

This study had a limitation in that it did not directly measure the amount of food consumed. FLIC, which measures fly-food interactions electronically, such as "licks", will also count accidental touches of food, including those not only with the proboscis but also the legs. Thus, theoretically, an increase in locomotor activity might also increase licks. While this possibility is certainly plausible, the data on locomotor activity show decreases in activity in WD-lineage offspring parallel to increases in licking. In future research, food preference and CAFÉ assays should be used to better understand feeding behavior. It would also be interesting to investigate how miR-10 overexpression may affect F1 feeding behavior.

# Conclusion

In conclusion, our data demonstrate that ancestral caloric overload led to reprogramming of feeding behavior in four successive generations of offspring. This is the first direct demonstration that ancestral diet can cause transgenerational transmission of food preferences. Although it is not yet clear whether similar effects are observable in human populations, the results of this study as well as familial clustering of obesity may indicate that children's food preferences and eating habits could be preconceptually hard-wired into the brain.

## Abbreviations

WD- western diet; CF- control diet fathers, EF- exercise fathers; WF- western diet fathers, WEF- western diet +exercise fathers; CFO- control diet father offspring, EFO- exercise father offspring, WFO- western diet father offspring, WEFO- western diet +exercise father offspring.

## Declarations

**Acknowledgments:** We thank undergraduate students Steven Bradley, Morgan Tedder, Damani Fitzgerald, Aaron Johnson, Imani Lowery, and Angela Sehres for technical assistance. We are very grateful to Dr. Kevin O'Brien (ECU) for his advice on statistical methods. This study was supported in parts NIEHS R15ES029673 (AKM) and NIH-NIGMS (KMB).

## References

1. Di Cesare, M., et al.: The epidemiological burden of obesity in childhood: a worldwide epidemic requiring urgent action. BMC Med. **17**, 212 (2019)
2. O'Brien, P.D., Hinder, L.M., Callaghan, B.C., Feldman, E.L.: Neurological consequences of obesity. Lancet Neurol. **16**, 465–477 (2017)
3. Donofry, S.D., Stillman, C.M., Erickson, K.I.: A review of the relationship between eating behavior, obesity and functional brain network organization. Soc. Cogn. Affect. Neurosci. **15**, 1157–1181 (2020)
4. Nielsen, L.A., Bojsoe, C., Kloppenborg, J.T., Trier, C., Gamborg, M., Holm, J.C.: The influence of familial predisposition to cardiovascular complications upon childhood obesity treatment. PLoS One. **10**, e0120177 (2015)
5. Li, Z., Luo, B., Du, L., Hu, H., Xie, Y.: Familial clustering of overweight and obesity among schoolchildren in northern China. Int. J. Clin. Exp. Med. **7**, 5778–5783 (2014)
6. Rohde, K., Keller, M., la Cour Poulsen, L., Bluher, M., Kovacs, P., Bottcher, Y.: Genetics and epigenetics in obesity. Metabolism. **92**, 37–50 (2019)
7. Llewellyn, C.H., Trzaskowski, M., Plomin, R., Wardle, J.: Finding the missing heritability in pediatric obesity: the contribution of genome-wide complex trait analysis. Int. J. Obes. (Lond). **37**, 1506–1509 (2013)

8. Silventoinen, K., Rokholm, B., Kaprio, J., Sorensen, T.I.: The genetic and environmental influences on childhood obesity: a systematic review of twin and adoption studies. Int. J. Obes. (Lond). **34**, 29–40 (2010)
9. Schulz, L.C.: The Dutch Hunger Winter and the developmental origins of health and disease. Proc. Natl. Acad. Sci. U S A. **107**, 16757–16758 (2010)
10. Lumey, L.H., Stein, A.D., Kahn, H.S., Romijn, J.A.: Lipid profiles in middle-aged men and women after famine exposure during gestation: the Dutch Hunger Winter Families Study. Am. J. Clin. Nutr. **89**, 1737–1743 (2009)
11. Bygren, L.O., Kaati, G., Edvinsson, S.: Longevity determined by paternal ancestors' nutrition during their slow growth period. Acta Biotheor. **49**, 53–59 (2001)
12. Kaati, G., Bygren, L.O., Edvinsson, S.: Cardiovascular and diabetes mortality determined by nutrition during parents' and grandparents' slow growth period. Eur. J. Hum. Genet. **10**, 682–688 (2002)
13. Perez, M.F., Lehner, B.: Intergenerational and transgenerational epigenetic inheritance in animals. Nat. Cell. Biol. **21**, 143–151 (2019)
14. King, S.E., Skinner, M.K.: Epigenetic Transgenerational Inheritance of Obesity Susceptibility. Trends Endocrinol. Metab. **31**, 478–494 (2020)
15. Dupont, C., Kappeler, L., Saget, S., Grandjean, V., Levy, R.: Role of miRNA in the Transmission of Metabolic Diseases Associated With Paternal Diet-Induced Obesity. Front. Genet. **10**, 337 (2019)
16. Isganaitis, E., Suehiro, H., Cardona, C.: Who's your daddy?: paternal inheritance of metabolic disease risk. Curr. Opin. Endocrinol. Diabetes Obes. **24**, 47–55 (2017)
17. Rando, O.J., Simmons, R.A.: I'm eating for two: parental dietary effects on offspring metabolism. Cell. **161**, 93–105 (2015)
18. Anderson, L.M., Riffle, L., Wilson, R., Travlos, G.S., Lubomirski, M.S., Alvord, W.G.: Preconceptional fasting of fathers alters serum glucose in offspring of mice. Nutrition. **22**, 327–331 (2006)
19. Murashov, A.K., et al.: Paternal long-term exercise programs offspring for low energy expenditure and increased risk for obesity in mice. FASEB J. **30**, 775–784 (2016)
20. Short, A.K., et al.: Exercise alters mouse sperm small noncoding RNAs and induces a transgenerational modification of male offspring conditioned fear and anxiety. Transl Psychiatry. **7**, e1114 (2017)
21. Carone, B.R., et al.: Paternally induced transgenerational environmental reprogramming of metabolic gene expression in mammals. Cell. **143**, 1084–1096 (2010)
22. Fullston, T., et al.: Paternal obesity initiates metabolic disturbances in two generations of mice with incomplete penetrance to the F2 generation and alters the transcriptional profile of testis and sperm microRNA content. FASEB J. **27**, 4226–4243 (2013)
23. Ng, S.F., Lin, R.C., Laybutt, D.R., Barres, R., Owens, J.A., Morris, M.J.: Chronic high-fat diet in fathers programs beta-cell dysfunction in female rat offspring. Nature. **467**, 963–966 (2010)

24. Lindsay, R.S., Dabelea, D., Roumain, J., Hanson, R.L., Bennett, P.H., Knowler, W.C.: Type 2 diabetes and low birth weight: the role of paternal inheritance in the association of low birth weight and diabetes. Diabetes. **49**, 445–449 (2000)
25. Wang, C., et al.: Association between parental history of diabetes and the incidence of type 2 diabetes mellitus differs according to the sex of the parent and offspring's body weight: A finding from a Japanese worksite-based cohort study. Prev. Med. **81**, 49–53 (2015)
26. Ost, A., et al.: Paternal diet defines offspring chromatin state and intergenerational obesity. Cell. **159**, 1352–1364 (2014)
27. Matzkin, L.M., Johnson, S., Paight, C., Markow, T.A.: Preadult parental diet affects offspring development and metabolism in Drosophila melanogaster. PLoS One. **8**, e59530 (2013)
28. Buescher, J.L., et al.: Evidence for transgenerational metabolic programming in Drosophila. Dis. Model. Mech. **6**, 1123–1132 (2013)
29. Valtonen, T.M., Kangassalo, K., Polkki, M., Rantala, M.J.: Transgenerational effects of parental larval diet on offspring development time, adult body size and pathogen resistance in Drosophila melanogaster. PLoS One. **7**, e31611 (2012)
30. Dew-Budd, K., Jarnigan, J., Reed, L.K.: Genetic and Sex-Specific Transgenerational Effects of a High Fat Diet in Drosophila melanogaster. PLoS One. **11**, e0160857 (2016)
31. Vijendravarma, R.K., Narasimha, S., Kawecki, T.J.: Effects of parental larval diet on egg size and offspring traits in Drosophila. Biol. Lett. **6**, 238–241 (2010)
32. Guida, M.C., et al.: Intergenerational inheritance of high fat diet-induced cardiac lipotoxicity in Drosophila. Nat. Commun. **10**, 193 (2019)
33. Bozler, J., Kacsoh, B.Z., Bosco, G.: Transgeneratonal inheritance of ethanol preference is caused by maternal NPF repression.Elife**8**, (2019)
34. Dasgupta, P., Sarkar, S., Das, A.A., Verma, T., Nandy, B.: Intergenerational paternal effect of adult density in Drosophila melanogaster. Ecol. Evol. **9**, 3553–3563 (2019)
35. Seong, K.H., et al.: Paternal restraint stress affects offspring metabolism via ATF-2 dependent mechanisms in Drosophila melanogaster germ cells. Commun. Biol. **3**, 208 (2020)
36. Palu, R.A.S., Praggastis, S.A., Thummel, C.S.: Parental obesity leads to metabolic changes in the F2 generation in Drosophila. Mol. Metab. **6**, 631–639 (2017)
37. Murashov, A.K., et al.: Preference and detrimental effects of high fat, sugar, and salt diet in wild-caught Drosophila simulans are reversed by flight exercise. FASEB Bioadv. **3**, 49–64 (2021)
38. Ro, J., Harvanek, Z.M., Pletcher, S.D.: FLIC: high-throughput, continuous analysis of feeding behaviors in Drosophila. PLoS One. **9**, e101107 (2014)
39. May, C.E., et al.: High Dietary Sugar Reshapes Sweet Taste to Promote Feeding Behavior in Drosophila melanogaster. Cell. Rep. **27**, 1675–1685e1677 (2019)
40. McLaughlin, K.L., Kew, K.A., McClung, J.M., Fisher-Wellman, K.H.: Subcellular proteomics combined with bioenergetic phenotyping reveals protein biomarkers of respiratory insufficiency in the setting of

proofreading-deficient mitochondrial polymerase. Sci. Rep. **10**, 3603 (2020)

41. McLaughlin, K.L., et al.: Novel approach to quantify mitochondrial content and intrinsic bioenergetic efficiency across organs. Sci. Rep. **10**, 17599 (2020)
42. Lesack, K., Naugler, C.: An open-source software program for performing Bonferroni and related corrections for multiple comparisons. J. Pathol. Inform. **2**, 52 (2011)
43. Benjamini, Y., Hochberg, Y.: Controlling the False Discovery Rate: A Practical and Powerful Approach to Multiple Testing. J. Roy. Stat. Soc.: Ser. B (Methodol.). **57**, 289–300 (1995)
44. Okuda, S., et al.: jPOSTrepo: an international standard data repository for proteomes. Nucleic Acids Res. **45**, D1107–D1111 (2017)
45. Deutsch, E.W., et al.: The ProteomeXchange consortium in 2017: supporting the cultural change in proteomics public data deposition. Nucleic Acids Res. **45**, D1100–D1106 (2017)
46. Ross, S.P., Baker, K.E., Fisher, A., Hoff, L., Pak, E.S., Murashov, A.K.: miRNA-431 Prevents Amyloid-beta-Induced Synapse Loss in Neuronal Cell Culture Model of Alzheimer's Disease by Silencing Kremen1. Front. Cell. Neurosci. **12**, 87 (2018)
47. Rooney, J.P., et al.: PCR based determination of mitochondrial DNA copy number in multiple species. Methods Mol. Biol. **1241**, 23–38 (2015)
48. Lang, P., Hasselwander, S., Li, H., Xia, N.: Effects of different diets used in diet-induced obesity models on insulin resistance and vascular dysfunction in C57BL/6 mice. Sci. Rep. **9**, 19556 (2019)
49. Higa, T.S., Spinola, A.V., Fonseca-Alaniz, M.H., Evangelista, F.S.: Comparison between cafeteria and high-fat diets in the induction of metabolic dysfunction in mice. Int. J. Physiol. Pathophysiol Pharmacol. **6**, 47–54 (2014)
50. Sampey, B.P., et al.: Cafeteria diet is a robust model of human metabolic syndrome with liver and adipose inflammation: comparison to high-fat diet. Obes. (Silver Spring). **19**, 1109–1117 (2011)
51. Shafat, A., Murray, B., Rumsey, D.: Energy density in cafeteria diet induced hyperphagia in the rat. Appetite. **52**, 34–38 (2009)
52. Jais, A., et al.: PNOC(ARC) Neurons Promote Hyperphagia and Obesity upon High-Fat-Diet Feeding. Neuron. **106**, 1009–1025e1010 (2020)
53. Leigh, S.J., Kendig, M.D., Morris, M.J.: Palatable Western-style Cafeteria Diet as a Reliable Method for Modeling Diet-induced Obesity in Rodents.J Vis Exp, (2019)
54. Murashov, A.K., et al.: Preference and detrimental effects of high fat, sugar, and salt diet in wild-caught Drosophila simulans are reversed by flight exercise.FASEB BioAdvances, (2020)
55. Chen, D., Li, X., Zhang, L., Zhu, M., Gao, L.: A high-fat diet impairs mitochondrial biogenesis, mitochondrial dynamics, and the respiratory chain complex in rat myocardial tissues. J. Cell. Biochem. **119**, 9602 (2018)
56. Fazzini, F., et al.: Association of mitochondrial DNA copy number with metabolic syndrome and type 2 diabetes in 14 176 individuals. J. Intern. Med. **290**, 190–202 (2021)

57. Leuthner, T.C., Hartman, J.H., Ryde, I.T., Meyer, J.N.: PCR-Based Determination of Mitochondrial DNA Copy Number in Multiple Species. Methods Mol. Biol. **2310**, 91–111 (2021)
58. Siino, V., et al.: Obesogenic Diets Cause Alterations on Proteins and Theirs Post-Translational Modifications in Mouse Brains. Nutr. Metab. Insights. **14**, 11786388211012405 (2021)
59. Godin, J.D., et al.: Huntingtin is required for mitotic spindle orientation and mammalian neurogenesis. Neuron. **67**, 392–406 (2010)
60. Zhang, S., Feany, M.B., Saraswati, S., Littleton, J.T., Perrimon, N.: Inactivation of Drosophila Huntingtin affects long-term adult functioning and the pathogenesis of a Huntington's disease model. Dis. Model. Mech. **2**, 247–266 (2009)
61. Neumuller, R.A., et al.: Mei-P26 regulates microRNAs and cell growth in the Drosophila ovarian stem cell lineage. Nature. **454**, 241–245 (2008)
62. Li, Y., Maines, J.Z., Tastan, O.Y., McKearin, D.M., Buszczak, M.: Mei-P26 regulates the maintenance of ovarian germline stem cells by promoting BMP signaling. Development. **139**, 1547–1556 (2012)
63. Rodgers, A.B., Morgan, C.P., Leu, N.A., Bale, T.L.: Transgenerational epigenetic programming via sperm microRNA recapitulates effects of paternal stress. Proc. Natl. Acad. Sci. U S A. **112**, 13699–13704 (2015)
64. Rodgers, A.B., Morgan, C.P., Bronson, S.L., Revello, S., Bale, T.L.: Paternal stress exposure alters sperm microRNA content and reprograms offspring HPA stress axis regulation. J. Neurosci. **33**, 9003–9012 (2013)
65. Licursi, V., Conte, F., Fiscon, G., Paci, P.: MIENTURNET: an interactive web tool for microRNA-target enrichment and network-based analysis. BMC Bioinform. **20**, 545 (2019)
66. Vlachos, I.S., et al.: DIANA-miRPath v3.0: deciphering microRNA function with experimental support. Nucleic Acids Res. **43**, W460–466 (2015)
67. Tehler, D., Hoyland-Kroghsbo, N.M., Lund, A.H.: The miR-10 microRNA precursor family. RNA Biol. **8**, 728–734 (2011)
68. Lund, A.H.: miR-10 in development and cancer. Cell. Death Differ. **17**, 209–214 (2010)
69. Wang, Z., et al.: Dynamic Epigenetic Regulation of miR-10 Family Governs the Caudalization of Floor Plate Neural Progenitors. Re:GEN Open. **1**, 117–129 (2021)
70. Rodgers, A.B., Bale, T.L.: Germ Cell Origins of Posttraumatic Stress Disorder Risk: The Transgenerational Impact of Parental Stress Experience. Biol. Psychiatry. **78**, 307–314 (2015)
71. Riemensperger, T., et al.: A single dopamine pathway underlies progressive locomotor deficits in a Drosophila model of Parkinson disease. Cell. Rep. **5**, 952–960 (2013)
72. Pak, E.S., Murashov, A.K.: Drosophila Passive Avoidance Behavior as a New Paradigm to Study Associative Aversive Learning.J Vis Exp, (2021)
73. Saben, J.L., et al.: Maternal Metabolic Syndrome Programs Mitochondrial Dysfunction via Germline Changes across Three Generations. Cell. Rep. **16**, 1–8 (2016)

74. Cormier, R.P.J., Champigny, C.M., Simard, C.J., St-Coeur, P.D., Pichaud, N.: Dynamic mitochondrial responses to a high-fat diet in Drosophila melanogaster. Sci. Rep. **9**, 4531 (2019)
75. Aw, W.C., et al.: Genotype to phenotype: Diet-by-mitochondrial DNA haplotype interactions drive metabolic flexibility and organismal fitness. PLoS Genet. **14**, e1007735 (2018)
76. Aw, W.C., Garvin, M.R., Melvin, R.G., Ballard, J.W.O.: Sex-specific influences of mtDNA mitotype and diet on mitochondrial functions and physiological traits in Drosophila melanogaster. PLoS One. **12**, e0187554 (2017)
77. Barron, J.C., Hurley, E.P., Parsons, M.P.: Huntingtin and the Synapse. Front. Cell. Neurosci. **15**, 689332 (2021)
78. Das, S., Bhattacharyya, N.P.: Huntingtin interacting protein HYPK is a negative regulator of heat shock response and is downregulated in models of Huntington's Disease. Exp. Cell. Res. **343**, 107–117 (2016)
79. Weyer, F.A., Gumiero, A., Lapouge, K., Bange, G., Kopp, J., Sinning, I.: Structural basis of HypK regulating N-terminal acetylation by the NatA complex. Nat. Commun. **8**, 15726 (2017)
80. Dickson, E., Soylu-Kucharz, R., Petersen, A., Bjorkqvist, M.: Hypothalamic expression of huntingtin causes distinct metabolic changes in Huntington's disease mice. Mol. Metab. **57**, 101439 (2022)
81. Liu, N., Han, H., Lasko, P.: Vasa promotes Drosophila germline stem cell differentiation by activating mei-P26 translation by directly interacting with a (U)-rich motif in its 3' UTR. Genes Dev. **23**, 2742–2752 (2009)
82. Rastegari, E., et al.: WD40 protein Wuho controls germline homeostasis via TRIM-NHL tumor suppressor Mei-p26 in Drosophila.Development**147**, (2020)
83. Saetrom, P., Snove, O. Jr., Rossi, J.J.: Epigenetics and microRNAs. Pediatr. Res. **61**, 17R–23R (2007)
84. Yin, J., Ren, W., Huang, X., Deng, J., Li, T., Yin, Y.: Potential Mechanisms Connecting Purine Metabolism and Cancer Therapy. Front. Immunol. **9**, 1697 (2018)
85. Cropley, J.E., et al.: Male-lineage transmission of an acquired metabolic phenotype induced by grand-paternal obesity. Mol. Metab. **5**, 699–708 (2016)

# Figures

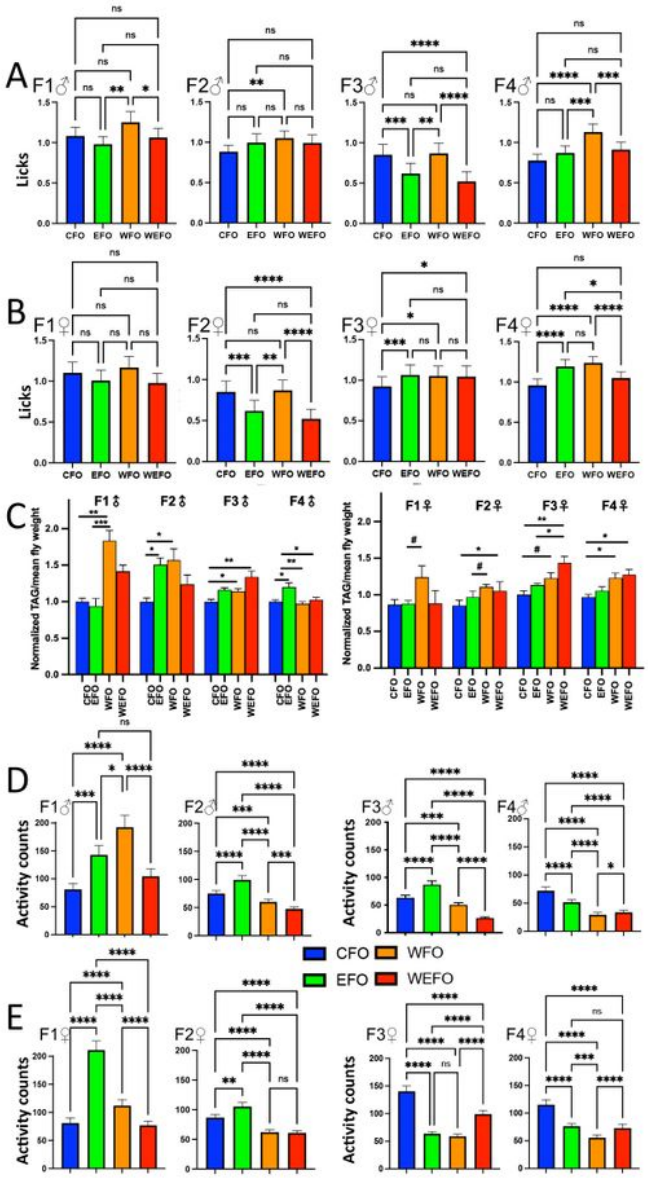


# Fig 1

## Figure 1

**Effects of ancestral diet and exercise on offspring feeding behavior, triglycerides and activity.**

**A.** Feeding activity of male offspring measured as "Licks" using FLIC. Flies were loaded into individual feeding chambers and consumption of 10% sucrose was measure over 24 h period starting at12pm. Each

group consisted of 9 flies (N=9). The graphs show successive generations from F1 to F4 from left to right. The experiments were repeated 3-4 times.

**B.** Feeding activity of female offspring measured in FLIC. The successive generations from F1 to F4 are shown from left to right. N=9. The experiments were repeated 3 times.

**C.** Whole body triglycerides. 3-4 day old flies were used for the analysis. Triglyceride content was normalized to mean fly weight. Left panel shows triglycerides in F1- F4 male flies. Right panel shows female offspring F1-F4. Five flies were used for each sample, N=5.

**D.** Locomotor activity of male offspring. The activity was measured over 5-day period in TriKinetics activity monitors in a climate-controlled environment at 24°C under a 12h light-dark cycle and 65-70 % humidity. Flies were housed in narrow vials with food in groups of 5. Y axis shows mean activity of 5 flies over 5-days. N= 12. The experiments were repeated 2-3times.

**E**. Locomotor activity of female offspring. Conditions, groups, and animal numbers are identical to those listed in legend D.

**Abbreviations:** CFO- CD father offspring, EFO- exercise father offspring, WFO- WD father offspring, WEFO- WD +exercise father offspring.

**Statistics.** Error bars represent SEM. Asterisk in panels A, B, D, E shows significance according to one-way ANOVA. A pairwise comparison was performed using Tukey's multiple comparisons test. In panel C, # indicates significance according to unpaired t-test. *- $P<0.05$, **- $P<0.01$, ***- $P<0.001$, ****- $P<0.0001$. #- $P<0.05$.

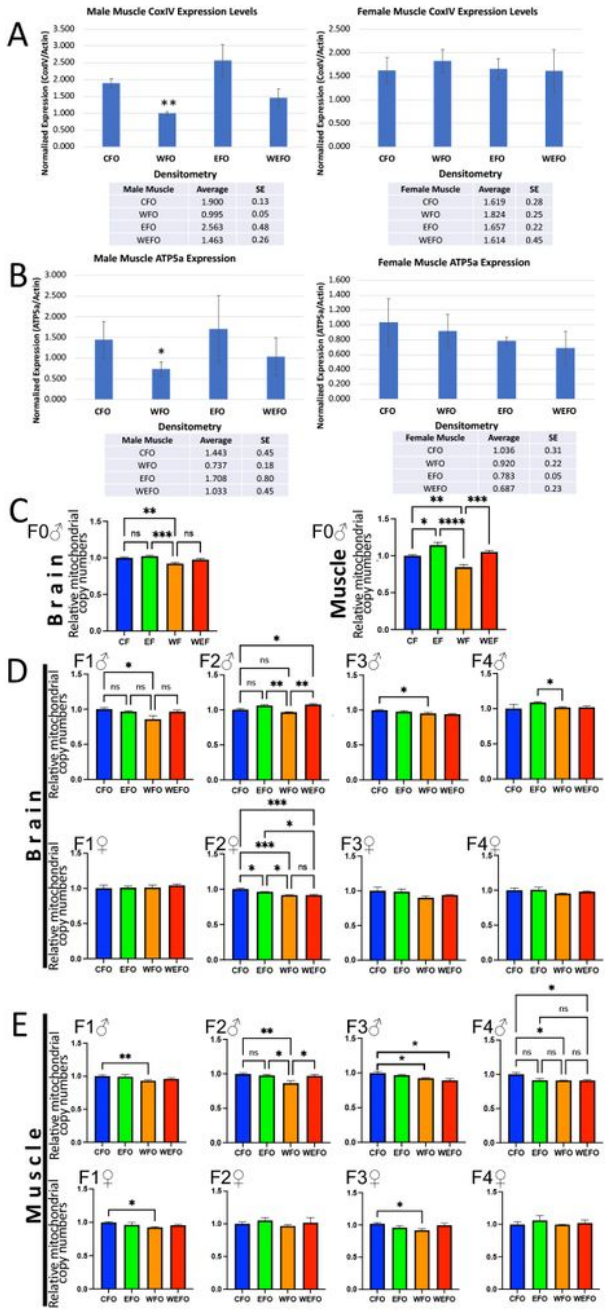


# Fig 2

## Figure 2

Effects of ancestral diet and exercise on mitochondrial enzymes and mitochondrial density.

**A.** Densitometry of CoxIV Western blots in flight muscles (for western blots see **SI Fig. 1**). Nitrocellulose membranes were probed with primary antibodies against CoxIV (Abcam). Expression was normalized

against actin. Histograms represent averages of three Western blot runs. **- P<0.01 indicates significance between WFO and CFO according to unpaired t-test.

**B.** Densitometry of ATP5a Western blots in flight muscles (for western blots see SI Fig. 1). All conditions are identical to those listed in legend A. *- P<0.05, indicates significance between WFO and CFO according to unpaired t-test.

**C.** Mitochondrial copy numbers in fathers' brains and muscles (F0). Abbreviations: CF- CD fathers, EF- exercise fathers; WF- WD fathers, WEF- WD +exercise fathers.

**D.** Mitochondrial copy numbers in offspring brains.

**E.** Mitochondrial copy numbers in offspring flight muscle.

Mitochondrial copy numbers were measured by qPCR of rpol2 (single-copy nDNA) and mt:lRNA (16S, mtDNA). Each sample contained DNA from five flight muscles or ten brains. Average of three experiments, n=9. One-way ANOVA, a pairwise comparison was performed using Tukey's multiple comparisons test. *- P<0.05, **- P<0.01, ***- P<0.001.

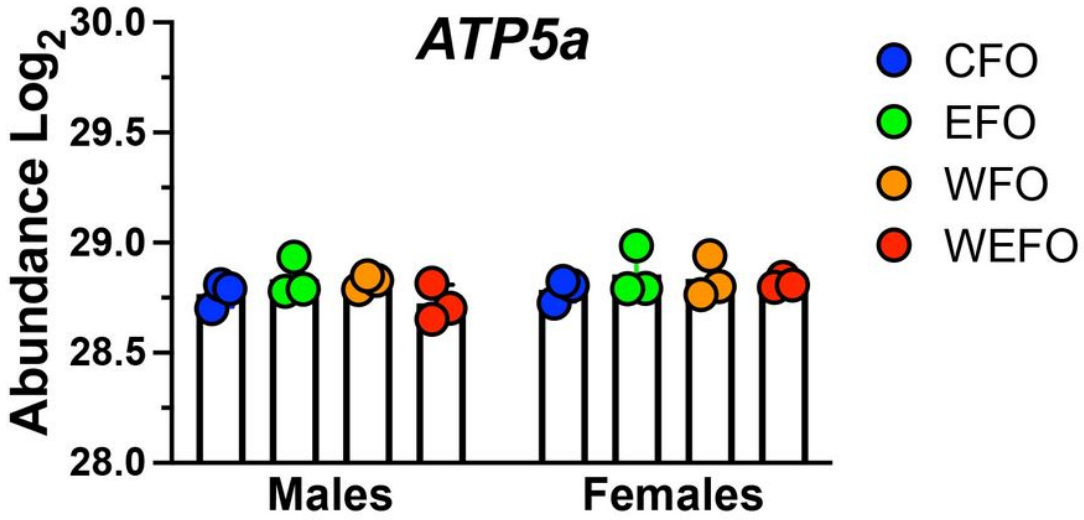


Fig. 6.

# Fig 3

## Figure 3

**Protein abundance of ATP5a synthase in the brain from F1 offspring**. All offspring lineages expressed the same abundance of ATP5a, confirming the same amount of protein in all samples. A total of 40 brains were sampled per group, N=3.

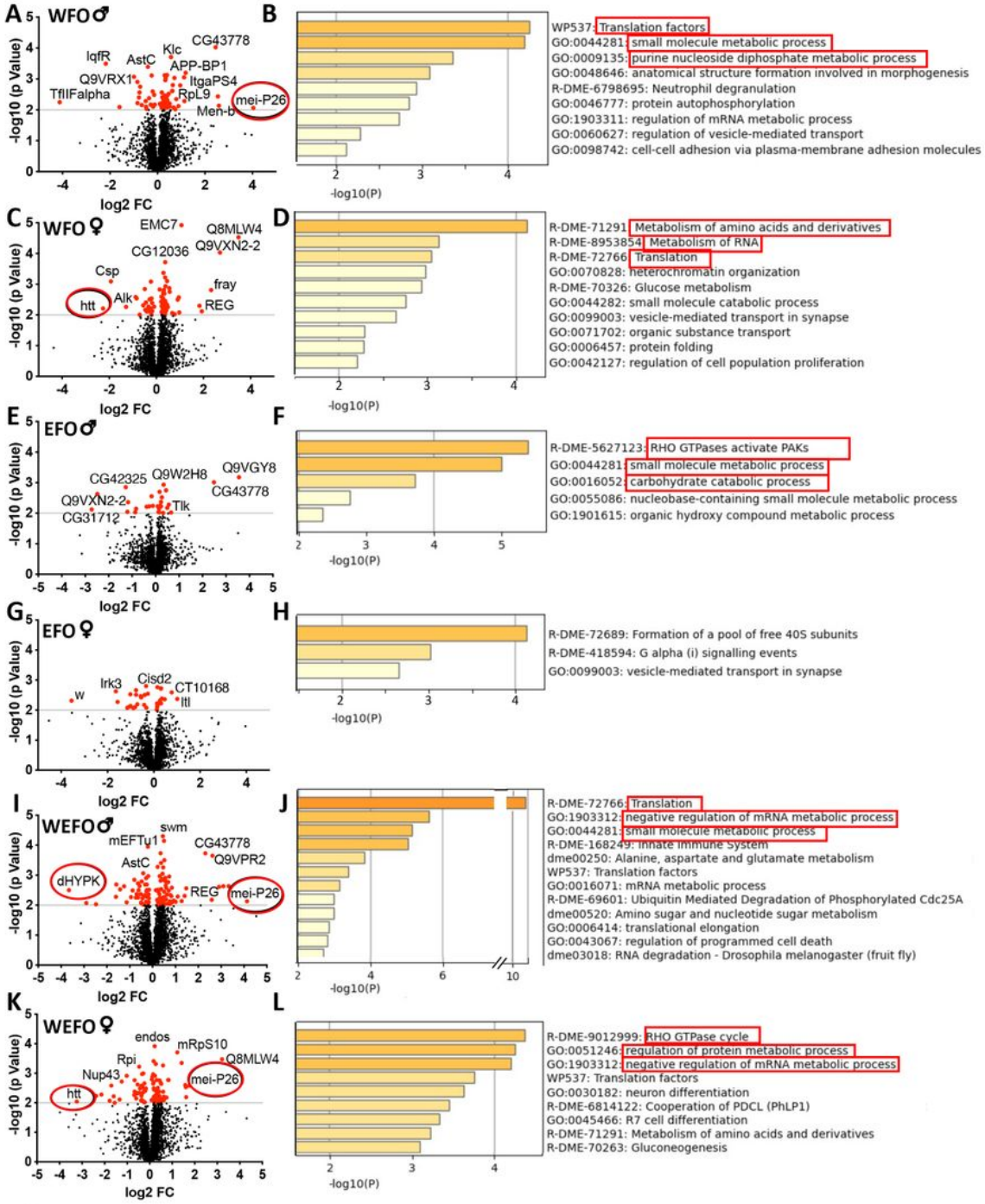


# Fig 4

## Figure 4

### Proteome analysis of the brains of F1 offspring by nLC-MS/MS.

**A.** Volcano plot depicting changes in the brain proteome between WFO and CFO males. Significance is indicated by the color and size of each circle, with 'significance' (p value <0.01) being represented by the

red circles. The encircled protein is mei-P26, which has been identified as being upregulated in several lineages. A total of 40 brains were sampled per group, N=3. The X-axis indicates fold change.

**B.** Metascape analysis of proteomic differences between WFO and CFO males. Bar plot shows significant enrichment in GO terms and pathways. The top three terms highlighted with red frames were translation factors, small molecule metabolism, and purine metabolism.

**C.** Volcano plot showing changes in the brain proteome between WFOs and CFO females. The encircled protein is htt, which has also been shown to be downregulated in female WEFOs. Graph parameters, experimental conditions, and N are the same as those listed in legend A.

**D.** Metascape analysis of proteomic differences between WFO and CFO females. Three major terms are highlighted with red frames.

**E.** Volcano plot showing changes in the brain proteome between EFOs and CFO males. Graph parameters, experimental conditions, and N are the same as those listed in legend A.

**F.** Metascape analysis of proteomic differences between EFO and CFO males.

**G**. Volcano plot showing changes in the brain proteome between EFOs and CFO females. Graph parameters, experimental conditions, and N are the same as those listed in legend A.

**H**. Metascape analysis of proteomic differences between EFO and CFO females.

**I.** Volcano plot showing changes in the brain proteome between WEFOs and CFO males. dHYPK, the encircled protein, is a partner of htt. Graph parameters, experimental conditions, and N are the same as those listed in legend A.

**J.** Metascape analysis of proteomic differences between WEFO and CFO males.

**K.** Volcano plot showing changes in the brain proteome between WEFOs and CFO females. Graph parameters, experimental conditions, and N are the same as those listed in legend A.

**L.** Metascape analysis of proteomic differences between WEFO and CFO females.

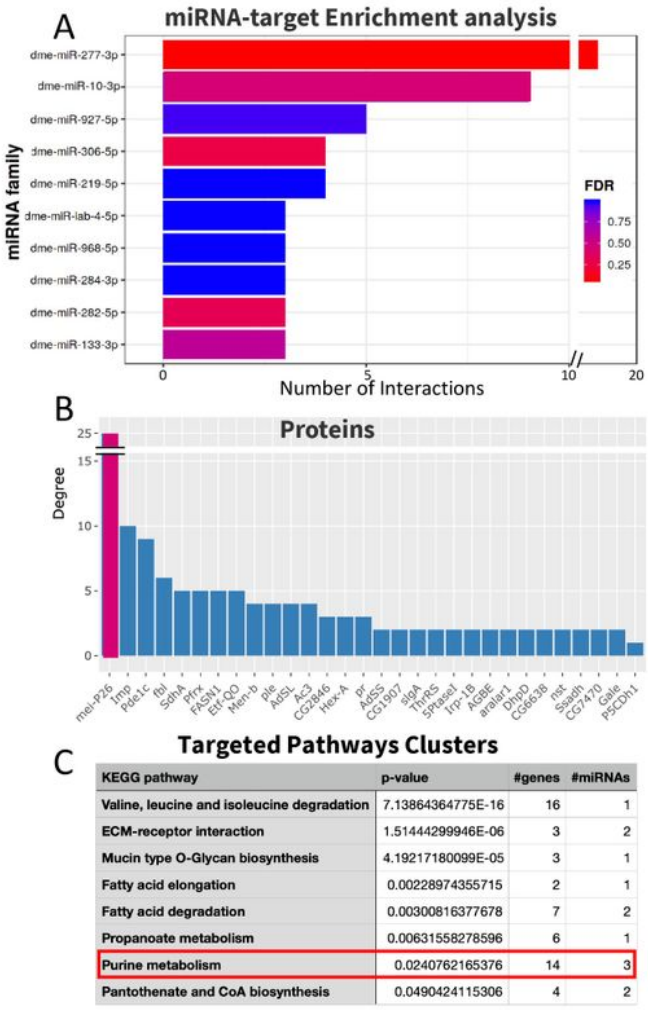


C

**Targeted Pathways Clusters**

| KEGG pathway | p-value | #genes | #miRNAs |
|---|---|---|---|
| Valine, leucine and isoleucine degradation | 7.13864364775E-16 | 16 | 1 |
| ECM-receptor interaction | 1.51444299946E-06 | 3 | 2 |
| Mucin type O-Glycan biosynthesis | 4.19217180099E-05 | 3 | 1 |
| Fatty acid elongation | 0.00228974355715 | 2 | 1 |
| Fatty acid degradation | 0.00300816377678 | 7 | 2 |
| Propanoate metabolism | 0.00631558278596 | 6 | 1 |
| Purine metabolism | 0.0240762165376 | 14 | 3 |
| Pantothenate and CoA biosynthesis | 0.0490424115306 | 4 | 2 |

**Fig 5**

## Figure 5

### MiRNA-target enrichment analysis of proteomic data.

**A.** Computational evidence of miRNA regulation on target genes based on a statistical analysis for over-representation of miRNA-target interactions. The Y-axis indicates the top ten miRNAs from the enrichment

analysis and the X-axis indicates how many proteins were targeted. The color code reflects the FDR value increasing from red to blue.

**B.** A bar plot of the mRNA degree, where X-axis refers to the first 30 target genes (sorted in a decreasing order according to the degree) and Y-axis refers to their degree (i.e., number of miRNA targeting them).

**C.** miRNA functional analyses using KEGG annotations using DIANA-tools mirPath. The results pane shows information regarding targeted pathways, p-values, as well as the number of miRNAs and genes present in each term. Red frame highlights purine metabolism, as a pathway targeted by all three miRNAs: mir-277-3p, mir-927-5p, and mir-10-3p.

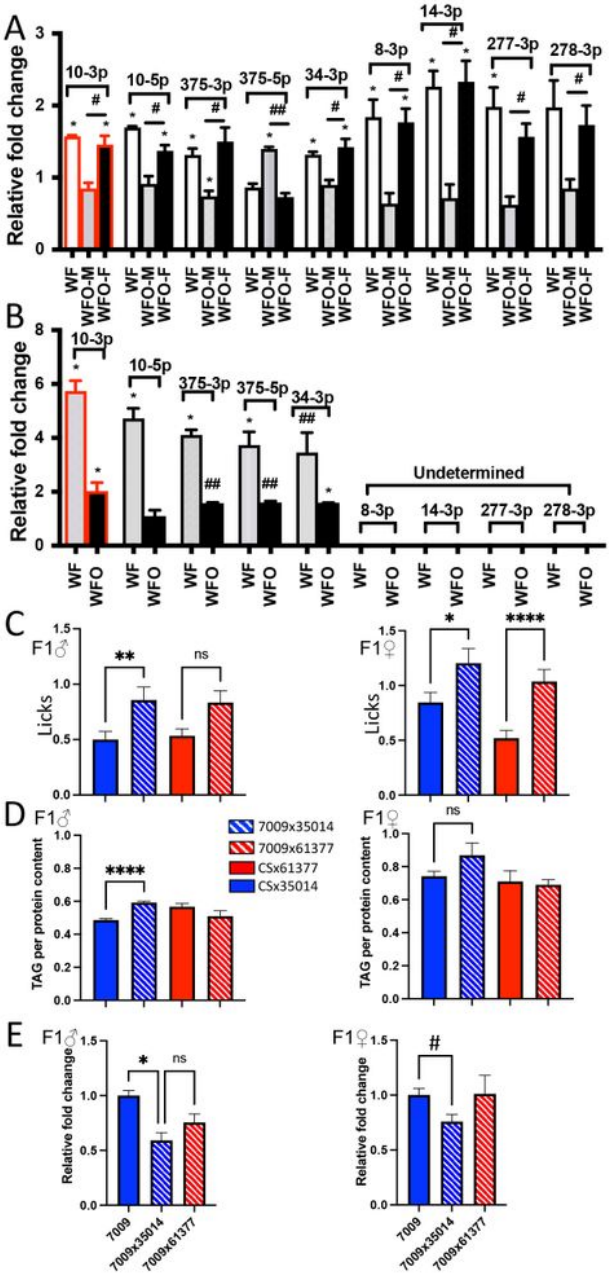


# Fig 6

## Figure 6

**Functional analyses miR-10 in modulating feeding behavior.**

**A.** MiRNA expression in the F0 and F1 brains. Relative fold change in comparison to CF and CFO taken as 1. WFO-M- WFO male offspring, WFO-F- WFO female offspring. Error bars represent SEM. Based on one-way ANOVA, the asterisks indicate significance when comparing WF to CF or WFO to CFO. A total of 10

brains were sampled per group, N=3. A pairwise comparison was performed using Tukey's multiple comparisons test. # Indicates significance according to unpaired t-test. *- P<0.05, #- P<0.05.

**B.** miRNA expression in F0 and F1 spermatozoa. in F0 spermatozoa. Relative fold change in comparison to CF and CFO taken as 1. Spermatozoa of 20 flies were pooled for each sample, N = 3. The asterisks indicate significance when comparing WF to CF or WFO to CFO based on one-way ANOVA. A pairwise comparison was performed using Tukey's multiple comparisons test. # Indicates significance according to unpaired t-test. *- P<0.05, #- P<0.05, ##- P< 0.01.

**C.** The effect of knocking down miR-10 in Ddc neurons on feeding behavior. Consumption of 10% sucrose was measure over 24 h period starting at12pm. Each group consisted of 9 flies (N=9). The experiments were repeated 3 times. One-way ANOVA, followed by Tukey's multiple comparisons test. *- P<0.05, **- P<0.01, ****- P<0.0001.

**D.** Effects of knockdown of miR-10 in Ddc neurons on whole body triglycerides (TAG). TAG content was normalized to protein per mean fly weight. Five flies were used for each sample, N=5. Asterisk indicates significance according to unpaired t-test. ****- P< 0.0001

**E.** qRT-PCR verification of miR-10 levels in mutant fly brains. Relative fold change in comparison to parental strain taken as 1. A total of 10 brains were sampled per group, N=3. One-way ANOVA followed by Tukey's multiple comparisons test, *- P<0.05. #- P<0.05 indicates significance according to unpaired t-test.

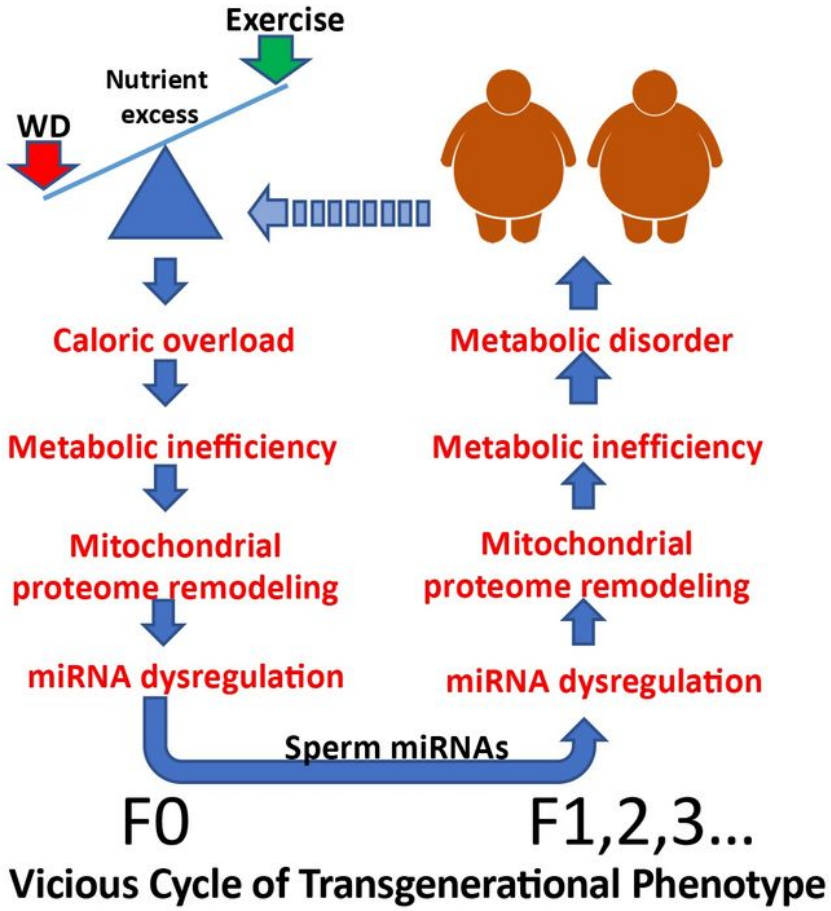


Fig 7

## Figure 7

Perfect vicious cycle of transgenerational phenotypes. As a result of caloric overload, metabolic efficiency is decreased, followed by proteome remodeling followed by dysregulation of miRNAs. Consequently, miRNAs serve as carriers of phenotypic information that transmits from generation to generation. A perfect vicious cycle is created when miRNAs influence development by altering proteomic function and

mitochondrial function, which leads to behavioral compensations such as overeating and a preference for energy-dense foods.

## Supplementary Files

This is a list of supplementary files associated with this preprint. Click to download.

- ProteomicDataMelanogasterProteins.xlsx
- SIFig.1.docx
- SIFig.23.docx